Figure 2

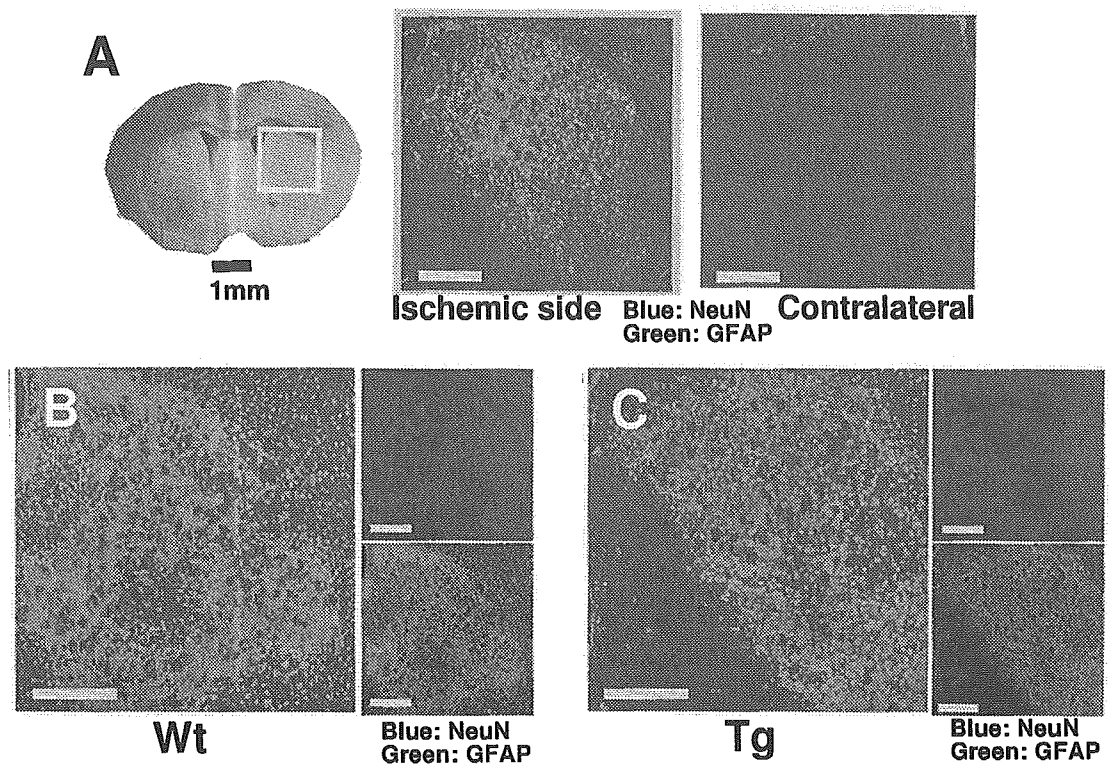
A
1mm
Ischemic side
Blue: NeuN
Green: GFAP
Contralateral
B
Wt
Blue: NeuN
Green: GFAP
C
Tg
Blue: NeuN
Green: GFAP
D
Infarct area (mm²/field)
1.2
1.0
0.8
0.6
0.4
0.2
0
ns
ns
*
*
*
Wt
Tg
Day0
Day3
Day7
Day28
Day56
E
Gliosis (mm²/field)
1.2
1.0
0.8
0.6
0.4
0.2
0
ns
ns
*
*
*
Wt
Tg
Day0
Day3
Day7
Day28
Day56

Figure 3

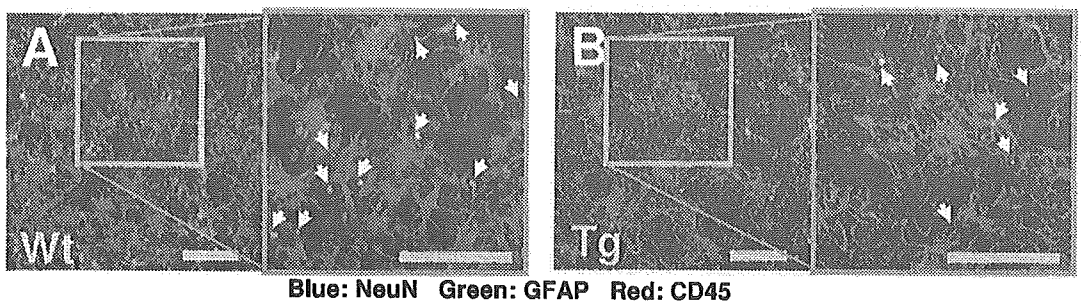

Blue: NeuN Green: GFAP Red: CD45

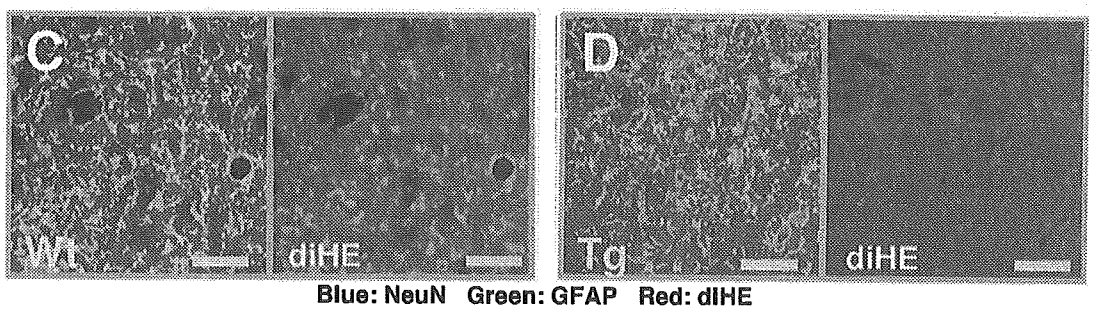

Blue: NeuN Green: GFAP Red: dIHE

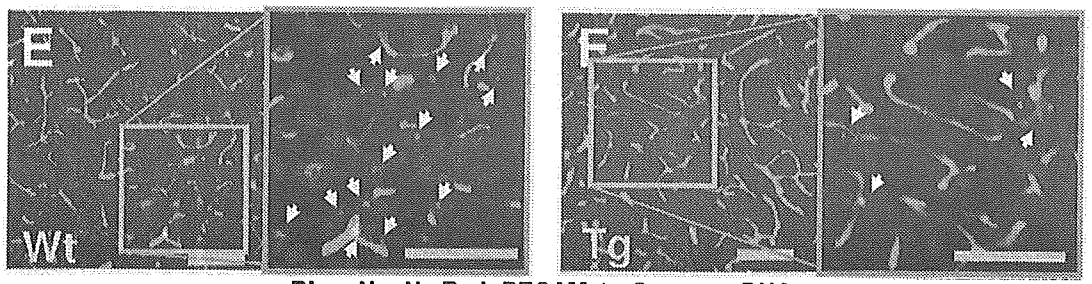

Blue: NeuN Red: PECAM-1 Green: ssDNA

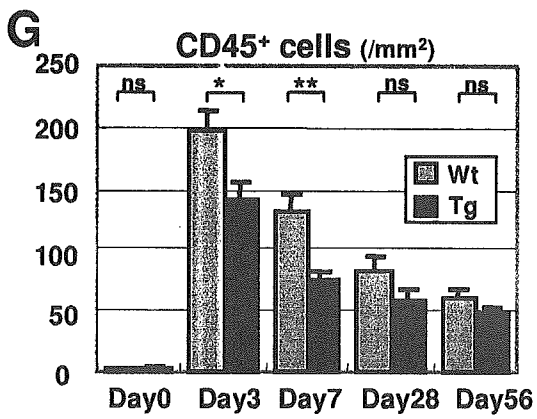

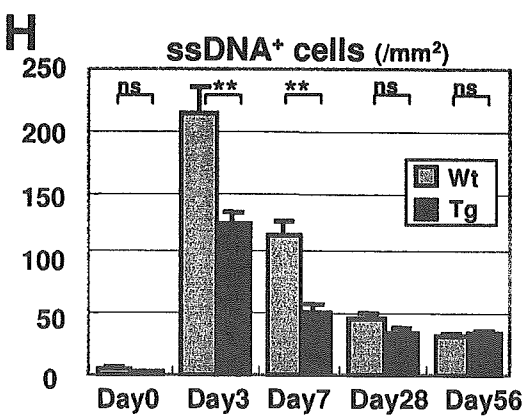

Figure 4

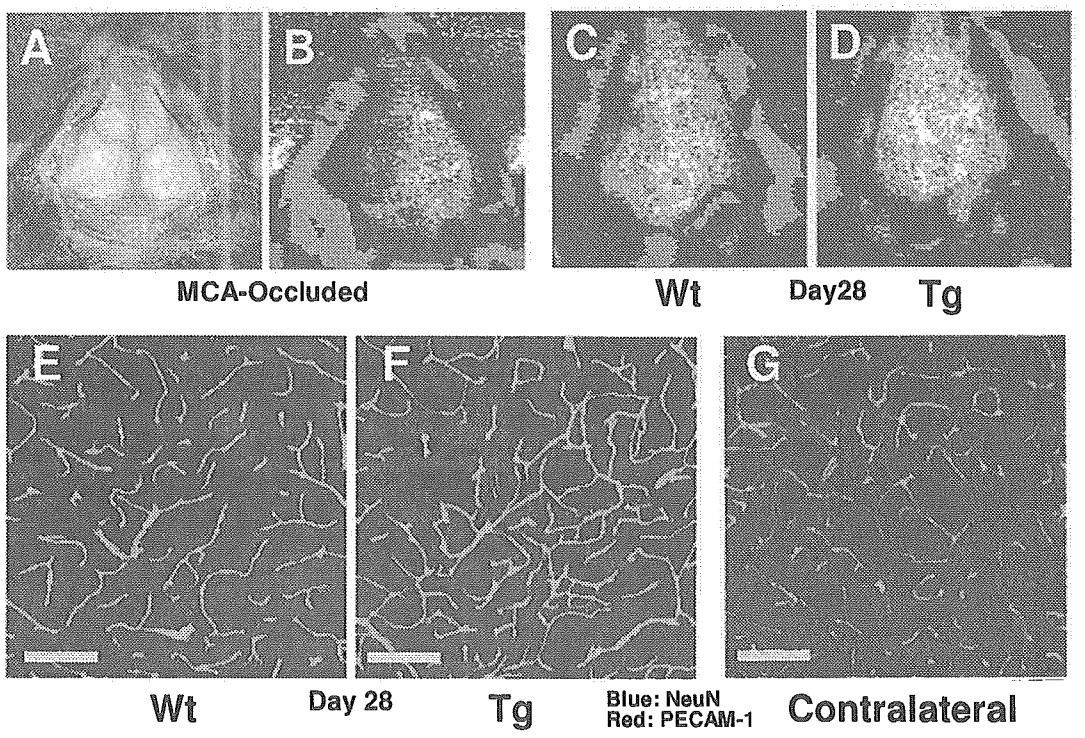
A
B
C
D
MCA-Occluded
Wt
Day28
Tg
E
F
G
Wt
Day 28
Tg
Blue: NeuN
Red: PECAM-1
Contralateral

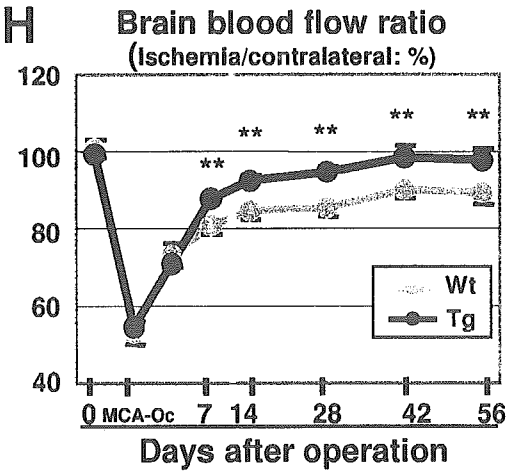
H
Brain blood flow ratio
(Ischemia/contralateral: %)
120
100
80
60
40
**
**
**
**
**
Wt
Tg
0 MCA-Oc
7
14
28
42
56
Days after operation

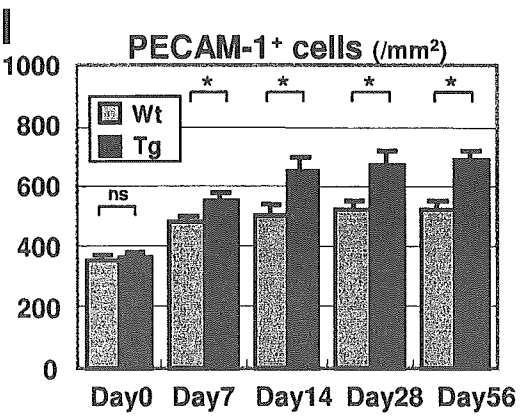
I
PECAM-1+ cells (/mm2)
1000
800
600
400
200
0
*
*
*
*
Wt
Tg
ns
Day0
Day7
Day14
Day28
Day56

Figure 5

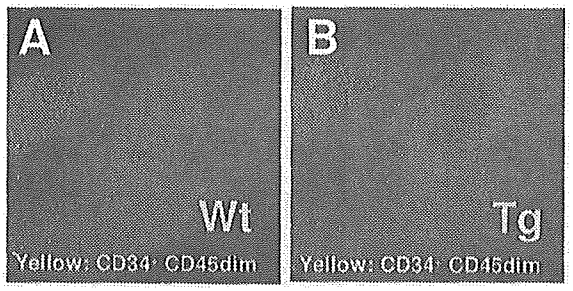
A
Wt
Yellow: CD34+ CD45dim
B
Tg
Yellow: CD34+ CD45dim

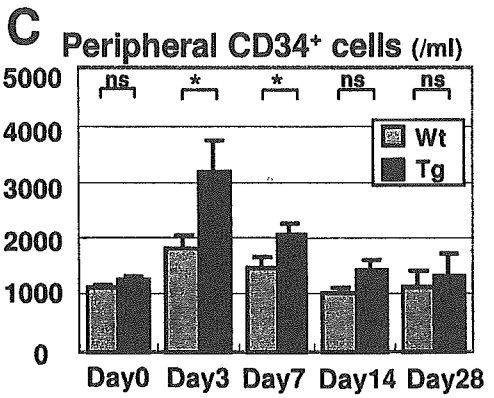
C
Peripheral CD34+ cells (/ml)
5000
4000
3000
2000
1000
0
ns
*
*
ns
ns
Wt
Tg
Day0
Day3
Day7
Day14
Day28

Figure 6

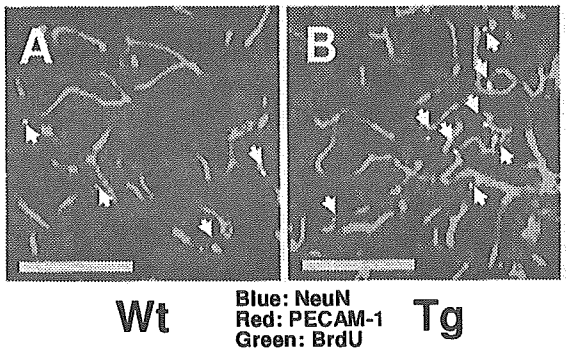
A
B
Wt
Blue: NeuN
Red: PECAM-1
Green: BrdU
Tg

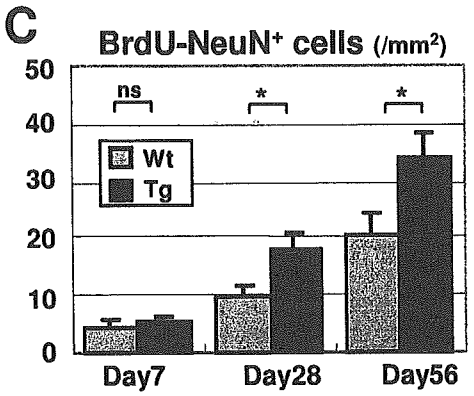
C
BrdU-NeuN+ cells (/mm2)
50
40
30
20
10
0
ns
*
*
Wt
Tg
Day7
Day28
Day56

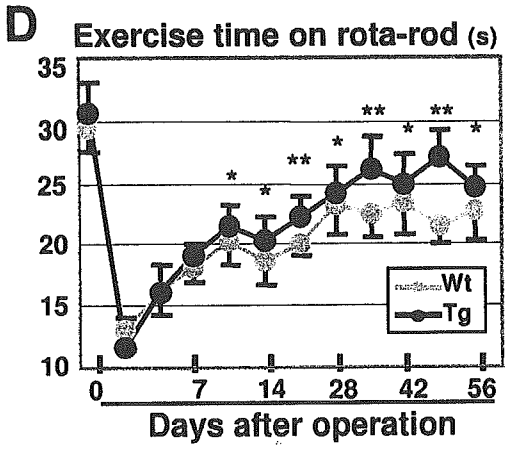
D
Exercise time on rota-rod (s)
35
30
25
20
15
10
0
7
14
28
42
56
Wt
Tg
Days after operation

Figure 7

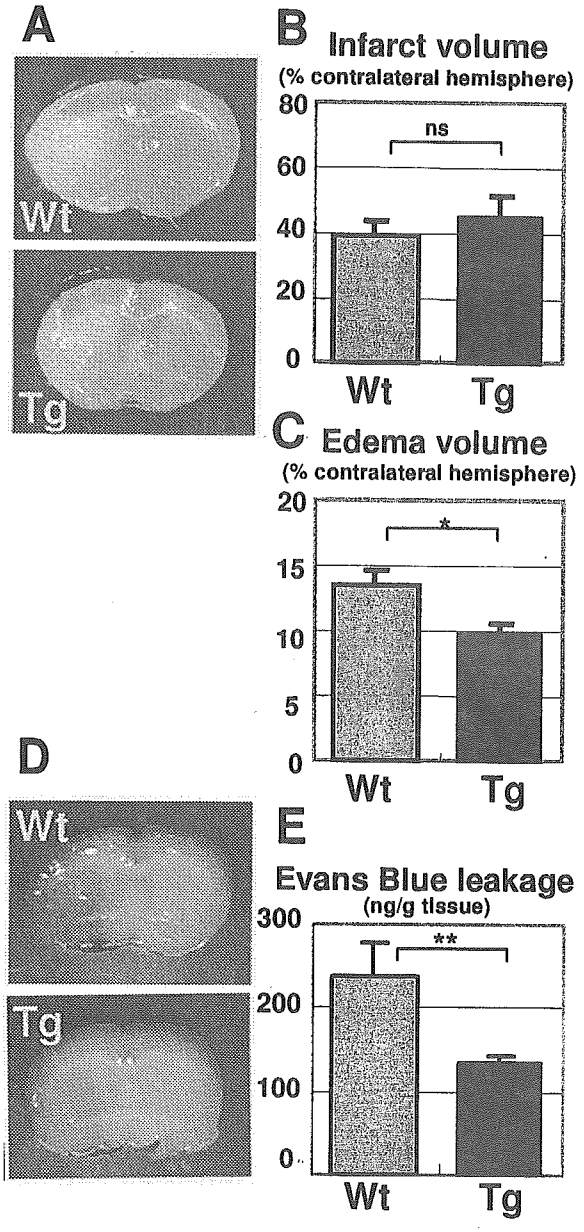
A
Wt
Tg
B
Infarct volume
(% contralateral hemisphere)
80
60
40
20
0
ns
Wt
Tg
C
Edema volume
(% contralateral hemisphere)
20
15
10
5
0
*
Wt
Tg
D
Wt
Tg
E
Evans Blue leakage
(ng/g tissue)
300
200
100
0
**
Wt
Tg

Figure 8

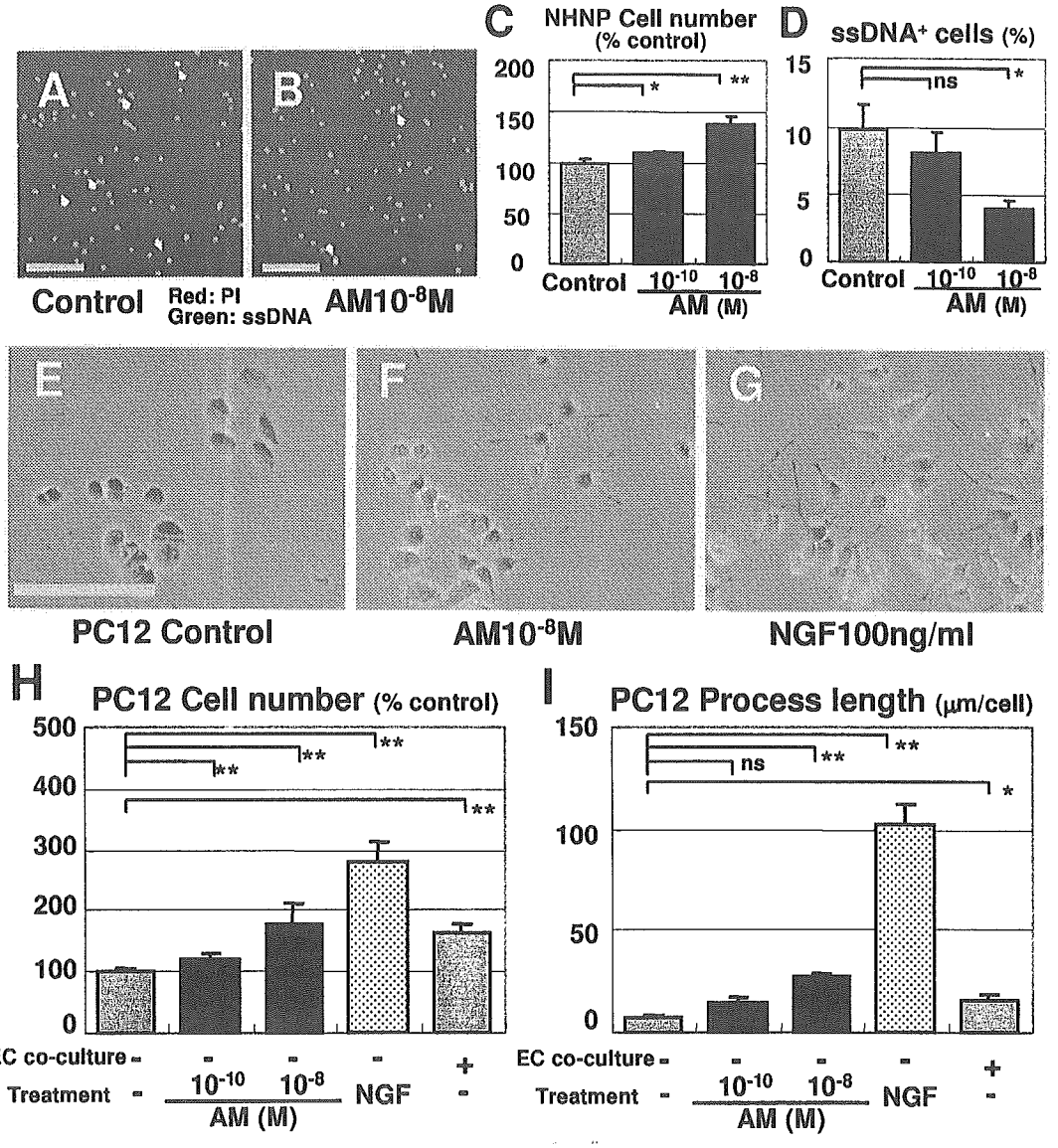
A
B
Control
Red: PI
Green: ssDNA
AM10-8M
C
NHNP Cell number
(% control)
200
150
100
50
0
*
**
Control
10-10
10-8
AM (M)
D
ssDNA+ cells (%)
15
10
5
0
ns
*
Control
10-10
10-8
AM (M)
E
F
G
PC12 Control
AM10-8M
NGF100ng/ml
H
PC12 Cell number (% control)
500
400
300
200
100
0
**
**
**
**
EC co-culture - - - - +
Treatment - 10-10 10-8 NGF -
AM (M)
I
PC12 Process length (μm/cell)
150
100
50
0
**
ns
**
*
EC co-culture - - - - +
Treatment - 10-10 10-8 NGF -
AM (M)

Figure 9

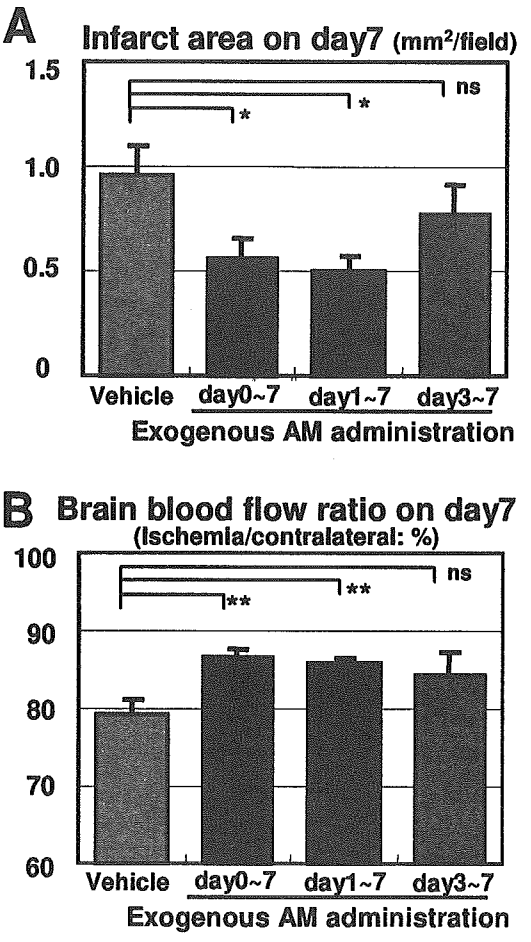
A
Infarct area on day7 (mm²/field)
1.5
1.0
0.5
0
ns
*
*
Vehicle
day0~7
day1~7
day3~7
Exogenous AM administration
B
Brain blood flow ratio on day7
(Ischemia/contralateral: %)
100
90
80
70
60
ns
**
**
Vehicle
day0~7
day1~7
day3~7
Exogenous AM administration

Figure 10

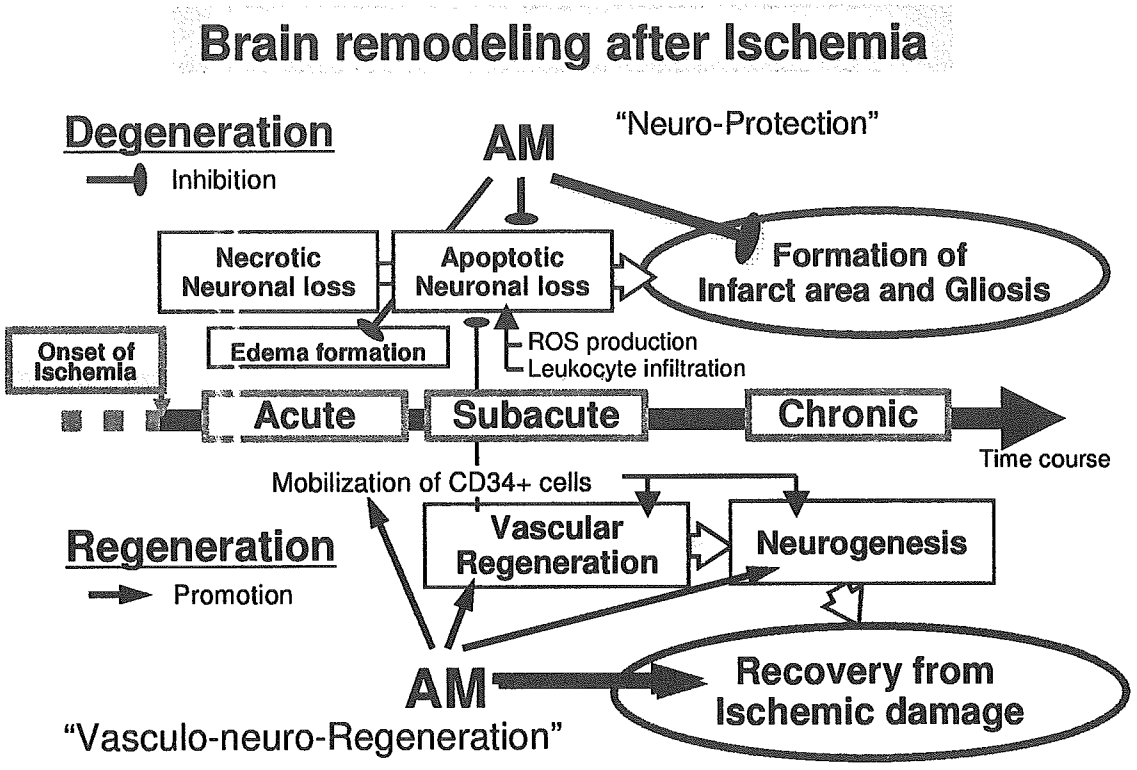
Brain remodeling after Ischemia
Degeneration
Inhibition
AM
"Neuro-Protection"
Necrotic Neuronal loss
Apoptotic Neuronal loss
Formation of Infarct area and Gliosis
Onset of Ischemia
Edema formation
ROS production
Leukocyte infiltration
Acute
Subacute
Chronic
Time course
Mobilization of CD34+ cells
Regeneration
Promotion
Vascular Regeneration
Neurogenesis
AM
Recovery from Ischemic damage
"Vasculo-neuro-Regeneration"

Notch/Rbp-j signaling prevents premature endocrine and ductal cell differentiation in the pancreas

Junji Fujikura,[1] Kiminori Hosoda,[1,*] Hiroshi Iwakura,[1] Tsutomu Tomita,[1] Michio Noguchi,[1] Hiroaki Masuzaki,[1] Kenji Tanigaki,[2] Daisuke Yabe,[2] Tasuku Honjo,[2] and Kazuwa Nakao[1]

[1] Department of Medicine and Clinical Science, Kyoto University Graduate School of Medicine, 54 Shogoin-Kawahara-cho, Sakyo-ku, Kyoto 606-8507, Japan
[2] Department of Medical Chemistry, Kyoto University Graduate School of Medicine, Yoshida-Konoe-cho, Sakyo-ku, Kyoto 606-8501, Japan
*Correspondence: pekopaokuro@yahoo.co.jp

Summary

To investigate the precise role of Notch/Rbp-j signaling in the pancreas, we inactivated Rbp-j by crossing Rbp-j floxed mice with *Pdx.cre* or *Rip.cre* transgenic mice. The loss of Rbp-j at the initial stage of pancreatic development induced accelerated α and PP cell differentiation and a concomitant decrease in the number of Neurogenin3 (Ngn3)-positive cells at E11.5. Then at E15, elongated tubular structures expressing ductal cell markers were evident; however, differentiation of acinar and all types of endocrine cells were reduced. During later embryonic stages, compensatory acinar cell differentiation was observed. The resultant mice exhibited insulin-deficient diabetes with both endocrine and exocrine pancreatic hypoplasia. In contrast, the loss of Rbp-j specifically in β cells did not affect β cell number and function. Thus, our analyses indicate that Notch/Rbp-j signaling prevents premature differentiation of pancreatic progenitor cells into endocrine and ductal cells during early development of the pancreas.

Introduction

The pancreas plays a key role in the maintenance of nutritional homeostasis through its exocrine and endocrine functions. The acini and ducts form the exocrine pancreas that produces and transports digestive enzymes into the duodenum. Besides, there are five known endocrine cell types in the pancreas: glucagon-producing α cells, insulin-producing β cells, somatostatin-producing δ cells, pancreatic polypeptide (PP)-producing PP cells, and ghrelin-producing ε cells (Heller et al., 2005).

Notch signaling regulates various developmental processes, such as neurogenesis, somitogenesis, angiogenesis, and hematopoiesis (Ishibashi et al., 1995; Hrabé de Angelis et al., 1997; Xue et al., 1999; Han et al., 2002). Interaction of a Notch receptor with its ligand induces cleavage of the receptor's intracellular domain (Notch ICD), which translocates to the nucleus and binds to Rbp-j to induce the expression of Hes family transcriptional repressors (Kageyama and Ohtsuka, 1999). Rbp-j is a key mediator of Notch signaling because it is expressed ubiquitously and associates with all four types of Notch receptors (Kato et al., 1996). Various Notch-related genes are expressed in the developing pancreas (Lammert et al., 2000). However, multiple anomalies and early embryonic lethalities of mice with homozygous deletions of genes such as *Dll1*, *Notch1*, *Notch2*, *Jagged1*, *Rbp-j*, or *Hes1* limits assessment of the importance of Notch/Rbp-j signaling in the pancreas (Swiatek et al., 1994; Ishibashi et al., 1995; Oka et al., 1995; Hrabé de Angelis et al., 1997; Apelqvist et al., 1999; Hamada et al., 1999; Xue et al., 1999; Jensen et al., 2000a). Although excess α cell differentiation in the pancreas has been reported at around E10 in mice with a generalized KO of Dll1 or Hes1 (Apelqvist et al., 1999; Jensen et al., 2000a), because β cells start to expand at around E13 and their differentiation occurs independently of α cells (Jensen et al., 2000b), the influence of Notch signaling on β cells remains to be elucidated. To address this issue, we created mice with developmental stage-specific deletion of *Rbp-j* in the pancreas using the Cre/loxP-mediated DNA recombination system.

Results

Accelerated premature differentiation of α and PP cells but not of β, δ, and ε cells in pancreatic Rbp-j KO (PRKO) mice

By crossing floxed Rbp-j (*Rbp-j$^{f/f}$*, designated as F/F) mice with *Pdx.cre* mice, we generated pancreatic Rbp-j KO (*Rbp-j$^{f/f}$ Pdx.cre*, designated as PRKO) mice (Gu et al., 2002; Han et al., 2002; see the Supplemental Data available with this article online). The *Pdx.cre* mouse begins to recombine loxP sites in the pancreatic epithelium before E9.5 (Figure S1B). Notch signaling negatively regulates proneural basic helix-loop-helix (bHLH) factors through Hes activation (Kageyama and Ohtsuka, 1999). A unique proendocrine bHLH transcription factor, Ngn3, is required for the development of pancreatic endocrine lineages (Gradwohl et al., 2000; Gu et al., 2002). We observed a premature increase in the number of Ngn3$^+$ cells in the pancreatic buds of PRKO mice (Figure S2A). At E11.5, a few scattered α cells among the protruding epithelial cells of F/F mice were observed (Figures 1E and 1E′). In PRKO mice, the number of α and PP cells increased and they surrounded the pancreatic buds (Figures 1F, 1F′, 1J, and 1J′). However, β, δ, and ghrelin-producing cell differentiation was not enhanced in the mutants (Figures 1D, 1D′, 1H, 1H′, and S3B). The number of Ngn3$^+$ cells decreased in PRKO mice compared with control mice (Figures 1M–1N′ and S2B). The number of proliferating cells detected by phosphohistone H3 (pHH3) immunostaining was comparable between control and mutant mice (Figures 1O–1P′). No apoptotic cells were

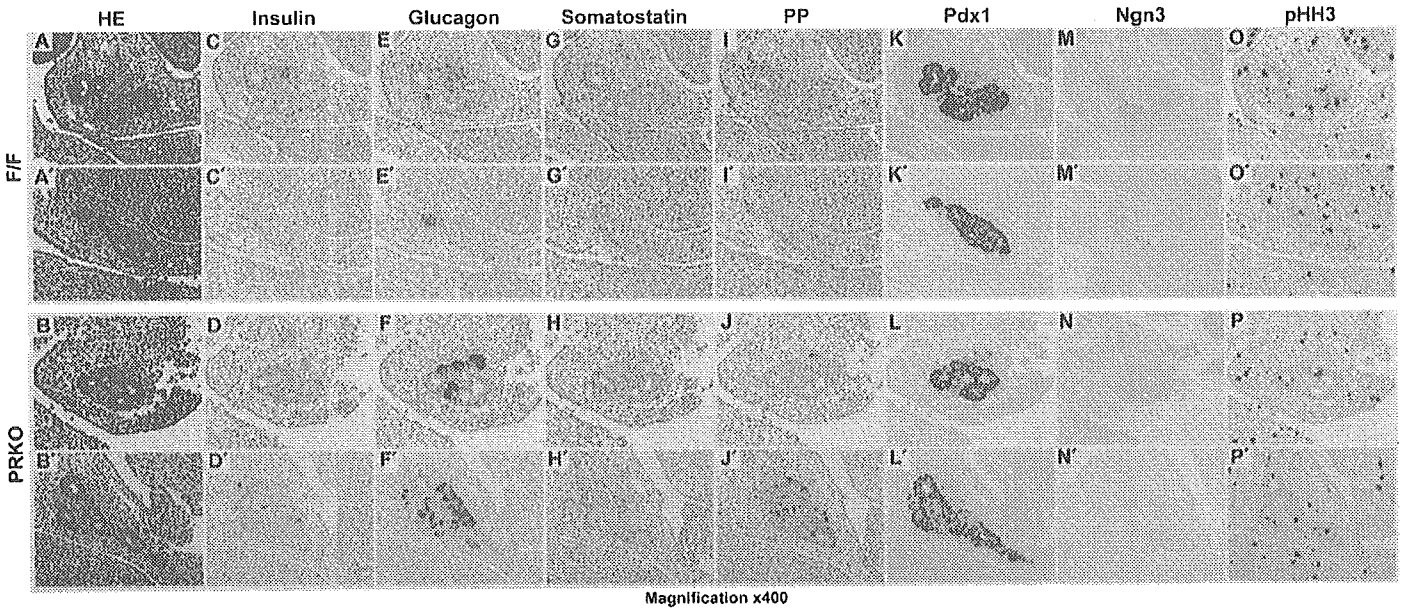

Figure 1. Accelerated premature differentiation of α and PP cells but not β, δ, and ε cells in pancreatic Rbp-j KO (PRKO) mice

A–P′) HE staining (**A–B′**), and immunostaining (**C–P′**) of representative serial pancreatic sections from F/F mice and PRKO mice at E11.5.

detected in the pancreatic epithelia of control or mutant mice (Figures S3C–S3E). These data indicate that earlier commitment to proendocrine ($Ngn3^+$) cells induced by defective Notch signaling results in precocious endocrine cell differentiation and a substantial loss of proendocrine cells during early pancreatic development.

Elongated tubular structures with decreased branching morphogenesis in the pancreas of the PRKO mouse

At E15, pancreatic $Pdx1^+$ epithelium of control mice exhibited complex and ramified networks (Figure 2B). However, in the mutant, branching of $Pdx1^+$ epithelium was severely impaired, and dilated tubular structures were prominent (Figure 2B′). The decreased epithelial branching was not associated with increased cell death or decreased proliferation, because these cells were not apoptotic (Figure 2D′), but exhibited active division (Figure 2M′). Moreover, acinar and β cells were scarcely differentiated (Figures 2C′ and 2H′), and aggregated α cells existed around the columnar tubular epithelium (Figure 2G′). The cells lining the lumens of tubular structures showed positive staining with cytokeratin (CK) and Dolichos biflorus agglutinin (DBA) lectin (Dor et al., 2004) (Figures 2K–2L′). The glucose transporter 2 (Glut2), expressed on the surface of differentiated β cells (Figure 2N), is also thought to be a marker of early pancreatic progenitor cells (Pang et al., 1994); however, Glut2 was not expressed in the tubular epithelium (Figure 2N′). In the control pancreas, *Hes1* expression was not detected (Figure 2O), but scattered $Ngn3^+$ cells were evident at this stage (Figure 2P). In the mutant pancreas, expression of *Hes1* and Ngn3 was virtually absent (Figures 2O′ and 2P′). ISL1 is a LIM homeodomain protein whose expression is initiated after Ngn3 extinction but before hormone production (Ahlgren et al., 1997). ISL1 expression was not detected in the tubular epithelium (Figure 2Q′). This analysis of various differentiation markers shows that the cells lining these tubular structures are not early progenitors, nor are they on the endocrine lineage. The tubular morphologies and high columnar epithelium resembling that of the large pancreatic duct rather suggest that the cells positive for ductal markers are duct cells. We confirmed that all of these cells were derived from Rbp-j-deficient cells by lineage tracing (Figure S4).

At later embryonic stages of PRKO mice, the acinar cell area was much smaller and CK^+ ductal cells occupied a larger area compared with F/F mice (Figures S5A–S5F). Although compensatory acinar growth was observed (Figures S5E–S5H), the interval sections revealed a much smaller pancreas in the mutant than in the control mouse (Figure S5I).

PRKO mice are born with pancreatic hypoplasia and exhibit insulin-deficient diabetes

The adult PRKO mouse exhibited a small pancreas (Figure 3A). The absolute pancreatic weight (PRKO, 209 ± 73 mg versus F/F, 685 ± 81 mg; $p = 0.0038$; Figure 3B) and the ratio of pancreatic weight to total body weight (data not shown) were lower in PRKO mice than in F/F mice. In pancreatic sections from PRKO mice, the number of islets per pancreas area was reduced (PRKO, 0.15 ± 0.06 versus F/F, 0.62 ± 0.13 islets/mm^2; $p = 0.015$; Figures 3C and 3D), and the size of the islets was smaller compared with F/F mice (Figure 3C). The relative endocrine cell mass was quantified by estimating the hormone-positive area per total pancreatic area in multiple pancreatic sections. The β cell mass of the PRKO mice was markedly reduced to about 25% of the β cell mass of F/F mice (PRKO, 0.21 ± 0.08% versus F/F, 1.13 ± 0.04%; $p < 0.001$; Figure 3E), and the absolute α cell mass was also significantly reduced to about 50% of that of the F/F mice (PRKO, 0.11 ± 0.02% versus F/F, 0.24 ± 0.02%; $p < 0.001$; Figure 3E). Total pancreatic insulin content (expressed per mg of pancreas weight) estimated from an acid-ethanol extract of the whole pancreas. PRKO mice had much lower insulin contents

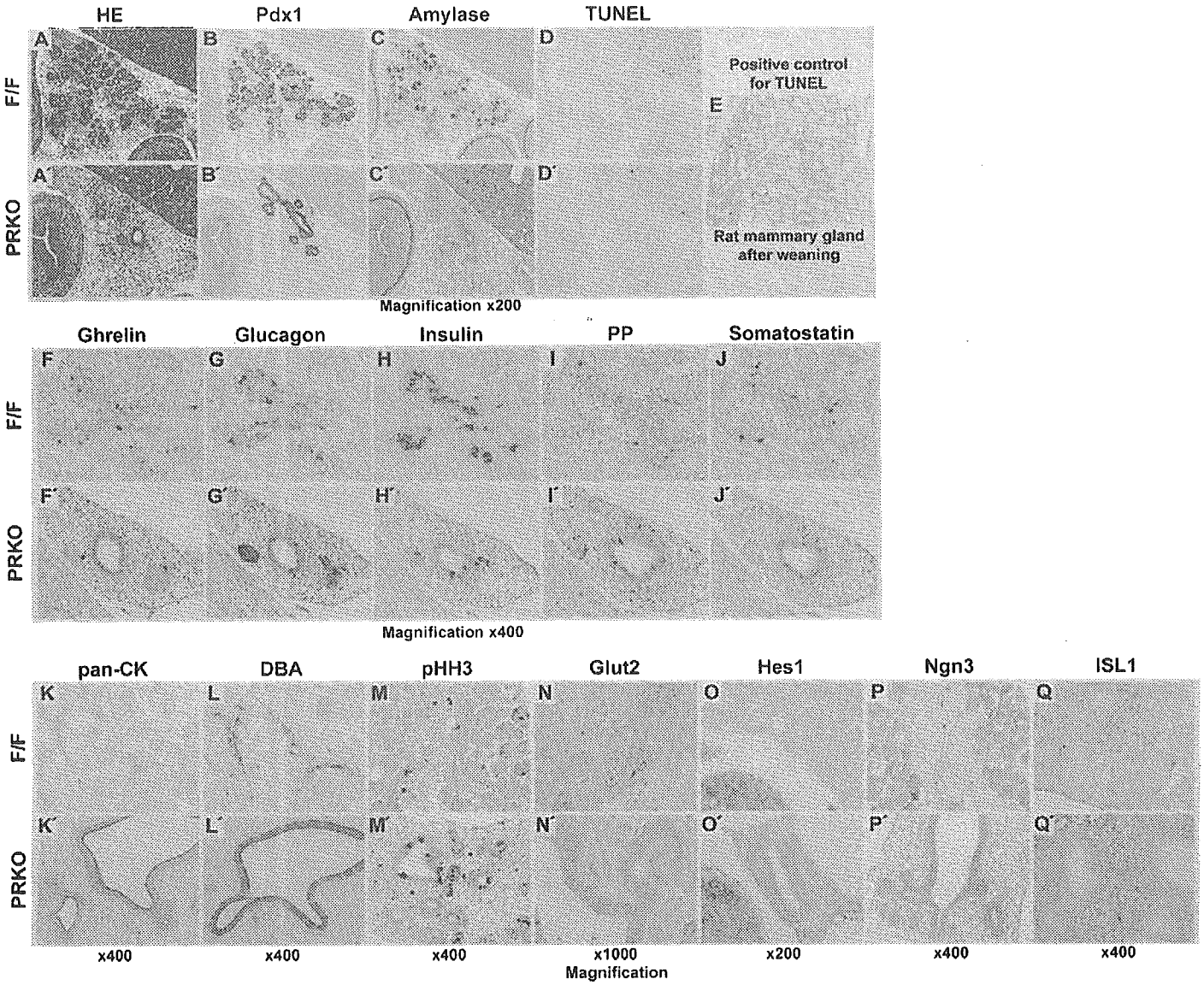

Figure 2. Elongated tubular structures with decreased branching in PRKO mice at E15

A–J′) Dilated and elongated duct-like structures in PRKO mice. HE staining (**A and A′**), immunostaining (**B–C′ and F–J′**), and TUNEL assay (**D and D′**) of serial pancreatic sections from F/F mice and PRKO mice at E15. The mammary gland of a postlactating female Wistar rat was used as a positive control for apoptosis (**E**).

K–Q′) Characterization of duct-like cells in PRKO mice. Immunostaining (**K–N′, P–Q′**) and *Hes1* in situ hybridization (**O and O′**) of pancreatic sections from F/F and PRKO mice at E15.

than the F/F mice (PRKO, 0.9 ± 0.2 pg/mg pancreas versus F/F, 96.4 ± 9.9 pg/mg pancreas; $p < 0.001$; Figure 3F). In addition to the scarcity of islets, histological analysis of the adult pancreas in PRKO mice revealed that the endocrine cells were frequently observed in association with distended pancreatic ducts (Figures 3J, 3L, 3N, 3P, and 3R). The relative ductal hyperplasia observed during the embryonic stages of PRKO mice (Figure S5D) became obscured in adult PRKO mice (Figure 3C).

The growth of PRKO mice and F/F mice fed normal chow was observed for four months. PRKO mice had a leaner phenotype than F/F mice and exhibited no further weight gain (Figures 3S and 3T). At eight weeks of age, PRKO mice developed significant hyperglycemia during fasting and feeding (fasting—PRKO, 348 ± 61 mg/dl versus F/F, 98 ± 6 mg/dl; $p < 0.001$; morning fed—PRKO, 524 ± 59 mg/dl versus F/F, 124 ± 12 mg/dl; $p < 0.001$; Figure 3U), which was accompanied by notably decreased plasma insulin concentrations (fasting—PRKO, below detection limit versus F/F, 0.48 ± 0.07 ng/ml; $p < 0.001$; morning fed—PRKO 0.04 ± 0.03 ng/ml versus F/F, 1.35 ± 0.25 ng/ml; $p = 0.0013$; Figure 3V). At this age, the mutant mice showed polyuria and polydipsia, and some appeared lethargic. Daily food intake increased in PRKO mice compared with control mice (PRKO, 8.3 ± 0.6 g/24 hr versus F/F, 4.1 ± 0.3 g/24 hr; $p < 0.001$; Figure 3W), which corresponded to diabetic hyperphagia. Thus, PRKO mice exhibited characteristics typical of diabetes with defective insulin secretion. Furthermore, PRKO mice had lower serum amylase activities than F/F mice (PRKO, 711 ± 58 U/dl versus F/F, 1121 ± 67 U/dl; $p = 0.0015$; Figure 3X), presumably due to pancreatic hypoplasia and severe diabetes.

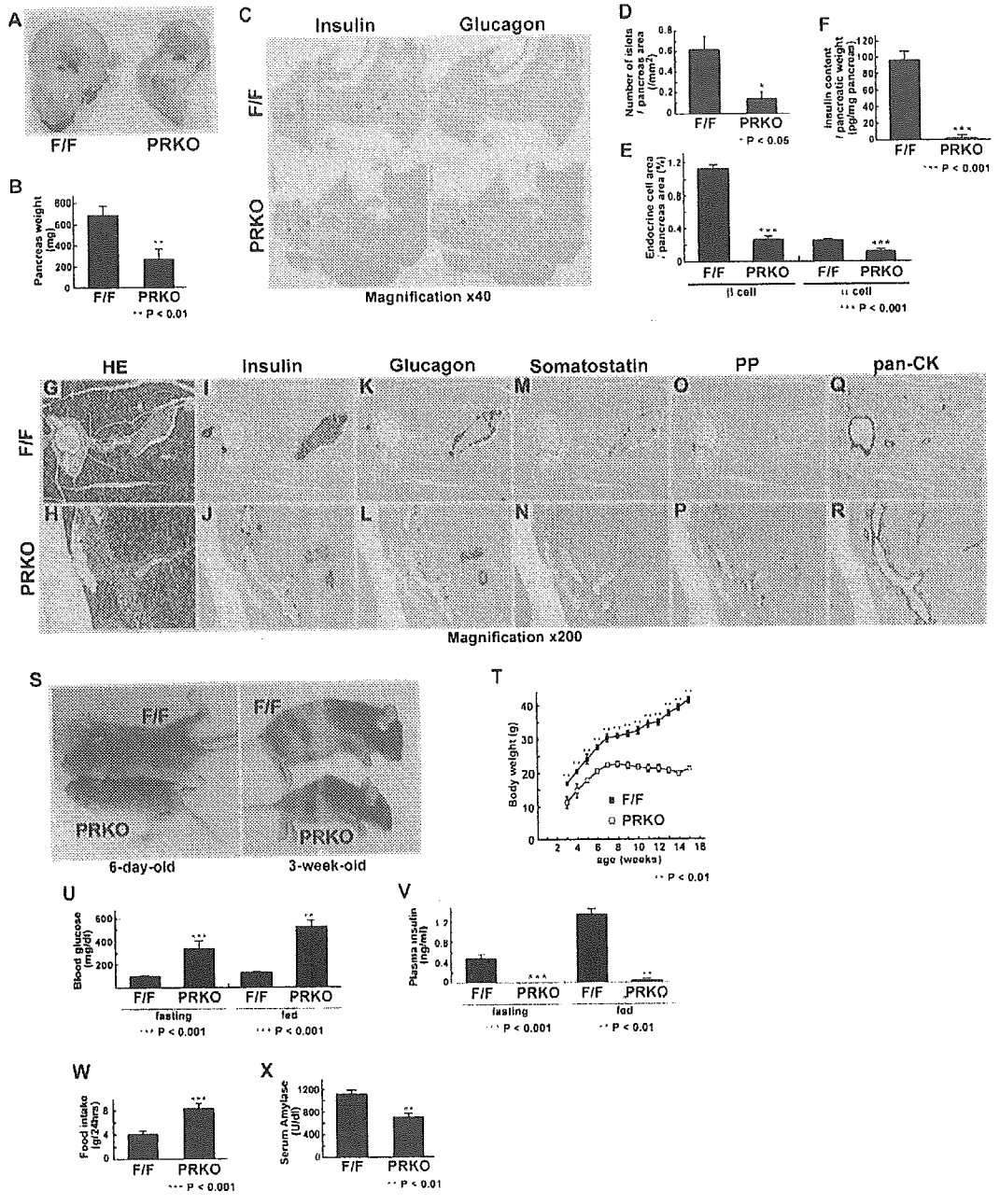

Figure 3. The adult PRKO mouse has a small pancreas, few islets, and low insulin content, which result in overt diabetes

A and B) Small pancreas in an adult PRKO mouse. Gut regions were dissected (**A**), and pancreatic weights were measured at 12 weeks of age (**B**).

C–E) Fewer islets and reduced endocrine cell mass in PRKO mice. Pancreatic sections from 10-week-old F/F mice and PRKO mice were immunostained for insulin and glucagon (**C**) to determine the number of islets (**D**), β cell area (**E**), and α cell area (**E**), which were normalized to total pancreatic area.

F) Lower pancreatic insulin content in PRKO mice. Pancreatic insulin content was measured in acid-ethanol extracts from 6-week-old F/F mice and PRKO mice.

G–R) Duct-associated endocrine cells in PRKO mice. HE staining (**G and H**) and immunostaining (**I–R**) of serial pancreatic sections from 8-week-old F/F and PRKO mice. The number of β cells was markedly reduced (**J**). Endocrine cells are located close to ductal structures (**J, L, N, and P**).

S and T) Growth retardation in PRKO mice. Gross appearances (**S**) of 6-day-old (left) and 3-week-old (right) PRKO mice (bottom) and control littermates (top). Growth curve (**T**) for litters obtained from mating F/F mice and PRKO mice.

U–W) Insulin-deficient diabetes in PRKO mice. Blood glucose concentrations (**U**) and plasma insulin concentrations (**V**) from fasted and random-fed 8-week-old male F/F mice and PRKO mice. Food intake (**W**) was measured for 24 hr from 16-week-old male F/F mice and PRKO mice.

X) Exocrine pancreatic insufficiency in F/F *Rip.cre* mice. Amylase activity was measured in serum from F/F mice and PRKO mice at 10 weeks of age.

Bars represent means ± SE of n = 4–8 mice. Levels of significance (Student's t test) are shown (*p < 0.05; **p < 0.01; ***p< 0.001).

β cell-specific Rbp-j KO (βRKO) mice have normal β cell number and function

By crossing F/F mice with *Rip.cre* mice, we next generated β cell-specific Rbp-j KO (*Rbp-j$^{f/f}$ Rip.cre*, designated as βRKO) mice (Figure S6). βRKO mice had normal body weight (βRKO, 35.2 ± 2.6 mg/dl versus *Rip.cre*, 37.0 ± 2.5 mg/dl; p = 0.62; Figure 4A). No significant differences were detected in the levels of blood glucose (βRKO, 160 ± 17 mg/dl versus *Rip.cre*,

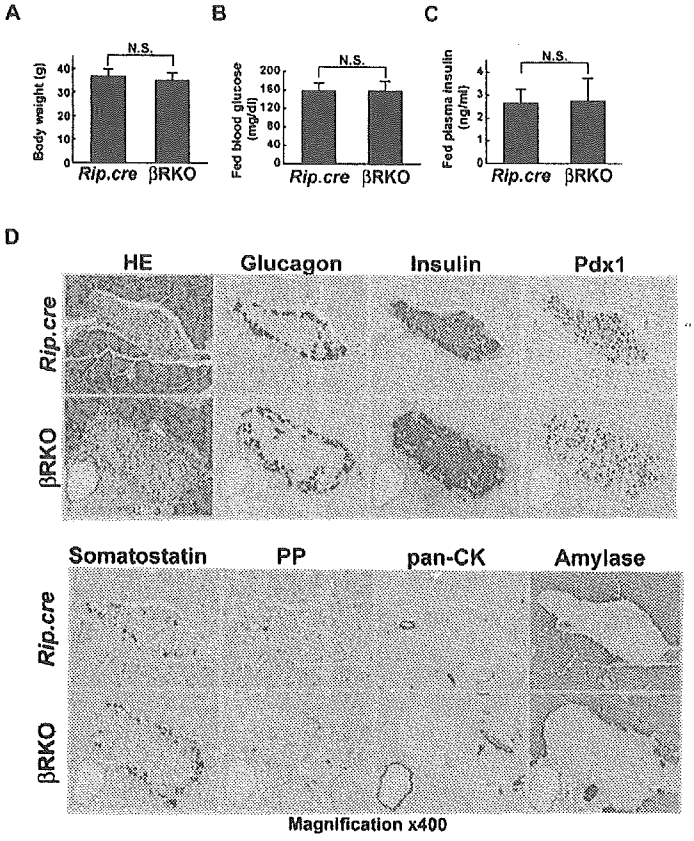

Figure 4. Absence of abnormalities in β cell-specific *Rbp-j* KO mice

A–C) Metabolic parameters of βRKO mice. Body weight (**B**), random-fed blood glucose concentrations (**C**), and random-fed plasma insulin concentrations (**D**) of 19-week-old male *Rip.cre* mice and βRKO mice.

D) Absence of morphological changes in the pancreas of the βRKO mouse. Immunohistochemistry of serial pancreatic sections of 20-week-old *Rip.cre* mice and βRKO mice.

Bars represent means ± SE of n = 7–8 mice. Levels of significance (Student's t test) are shown (NS, not significant).

159 ± 15 mg/dl; p = 0.95; Figure 4B) or plasma insulin (βRKO, 2.78 ± 1.10 ng/ml versus *Rip.cre*, 2.67 ± 0.55 ng/ml; p = 0.92; Figure 4C) in the fed state. Hematoxylin-eosin (HE) staining and immunohistochemical studies with glucagon, insulin, Pdx1, somatostatin, PP, pan-CK, and amylase revealed no abnormalities (Figure 4D). These data indicate that Rbp-j is not required for maintaining β cell function or β cell mass.

Discussion

Using the stage-specific conditional gene targeting approach, we documented the effects of Notch/Rbp-j signaling on pancreatic development and function.

Normally, Ngn3 expression peaks between E13.5 and E15.5 (Apelqvist et al., 1999). In PRKO mice, Ngn3 expression peaked at E10.5 and then declined at E11.5 (Figure 1), which suggests that termination of Notch signaling results in earlier commitment to endocrine cell lineages and earlier loss of endocrine progenitor cells. Before E12.5, the majority of endocrine cells formed are α and PP cells, and a wave of β and δ cell generation occurs after E13 (Pictet and Rutter, 1972; Murtaugh and Melton, 2003). In PRKO mice, α and PP cell differentiation was enhanced at E11.5, but β and δ cell differentiation was not enhanced. It was recently reported that Ngn3 protein transduction to E11.5 pancreatic cells resulted in α cell differentiation, but the transduction to E15 cells resulted in β cell differentiation (Dominguez-Bendala et al., 2005). In agreement with that report, our findings suggest that E11 proendocrine cells may lack some factor that contributes to β or δ cell differentiation.

Tubular structures with CK^+ DBA^+ cells dominated in the pancreas of the PRKO mouse at later embryonic stages (Figure 2). Thus, residual $Pdx1^+$ epithelial cells that have not undergone endocrine cell differentiation have a tendency to differentiate into ductal cells. A study demonstrated that genes that participate in the Notch pathway are upregulated in the metaplastic ductal epithelium of pancreatic premalignant legions (Miyamoto et al., 2003). Lineage-tracing studies show that ductal lineage is separated from $Pdx1^+$ $Ngn3^-$ common pancreatic progenitor cells between E9.5 and E12.5 (Gu et al., 2002); those are the times when the disruption of *Rbp-j* genes in PRKO mice occurs. These findings suggest that the appropriate downregulation of Notch signaling is necessary for pancreatic duct cell identity.

In the mutant mouse, the number of Pdx1-positive cells clearly decreased before E15 and the pancreas was small thereafter (Figures 2B′, 3A, and 3B). If the role of Notch signaling is simply to regulate cell fate, hypoplasia of certain types of cell should be accompanied by hyperplasia of other types of cell. For instance, in the determination of T and B lymphocytes, loss of function of Notch1 resulted in blockade of T cell development and enhancement of B cell production, while overexpression of Notch1 resulted in blockade of B cell lymphopoiesis and the generation of T cells (Pui et al., 1999; Wilson et al., 2001). The small pancreas and altered pancreatic cell composition in our mutant mouse suggest that defective Notch signaling allows premature differentiation of α, PP, and duct cells at the expense of later differentiating β, δ, and acinar cells. This mode of regulation is reminiscent of neuronal differentiation, in which Notch/Rbp-j signaling acts as a gatekeeper between self-renewal and commitment (Ishibashi et al., 1995).

In PRKO mice, though inadequate, the differentiation and growth of acinar cells occurred after E15. Persistent Notch ICD expression in pancreatic epithelium has been shown to inhibit acinar cell differentiation (Hald et al., 2003; Esni et al., 2004), and generalized Hes1 KO mice showed increased acinar cell growth (Jensen et al., 2000a). These results also suggest that Notch signaling inhibits acinar cell differentiation and proliferation during later embryonic stages.

The role of Notch signaling in terminally differentiated cells is unknown, although it was speculated that Notch might confer some degree of plasticity on postmitotic neurons (Ahmad et al., 1995). We detected the expression of Notch2 and Dll1 in endocrine cells of adult mice (data not shown). Furthermore, $Ngn3^+$ endocrine progenitor cells were shown to reside within the pancreatic islets (Gu et al., 2002); however, we found no difference between βRKO mice and control mice (Figure 4). It was reported that the β cells in adult islets are mainly formed by self-duplication of preexisting β cells and that the forced expression of Notch1 ICD in the adult pancreas does not perturb mature endocrine cells (Murtaugh et al., 2003; Dor et al., 2004). Together with the results of PRKO mice, Notch signaling may be indispensable only during the early developmental stages of the pancreas.

Our data show that Rbp-j is a key molecule in the propagation of pancreatic progenitor cells and is essential for proper differentiation into mature pancreatic cells.

Experimental procedures

Generation of pancreas- or β cell-specific Rbp-j KO mice

The generations of mice bearing a floxed allele of *Rbp-j* have been described previously (Han et al., 2002). *Pdx.cre* mice in which Cre recombinase is under the transcriptional control of the mouse Pdx1 promoter were gifts from Dr. Douglas A. Melton (Gu et al., 2002). *Rip.cre* mice in which Cre recombinase is under the control of the rat insulin II promoter were purchased from the Jackson Laboratory. Mice homozygous for the floxed *Rbp-j* allele (F/F) were crossed with *Pdx.cre* or *Rip.cre* transgenic mice. The resultant double-heterozygous mice were then crossed with *Rbp-j*$^{f/+}$ mice, resulting in *Rbp-j*$^{f/f}$ *Pdx.cre* (PRKO) or *Rbp-j*$^{f/f}$ *Rip.cre* (βRKO) mice and their control littermates. Genotyping and assessment of deletion efficiency were performed by Southern blot analyses on genomic DNA obtained from tails or other tissues.

Histological analyses

Whole embryos or excised pancreas were fixed with 4% paraformaldehyde in PBS for overnight at 4°C then paraffin embedded, and 5 μm sections were cut and mounted on glass slides. Slides were dewaxed, rehydrated, and, in some instances, subjected to antigen retrieval by autoclaving at 121°C for five minutes with 10 mM citrate buffer. Endogenous peroxidase was inactivated with 0.3% H_2O_2 in methanol for 30 min. The slides were blocked for 1 hr with a reagent containing casein (DAKO Protein Block Serum-Free Solution; Dako), then stained overnight with the following primary antibodies (Abs): rabbit anti-Pdx1 (Guz et al., 1995), rabbit anti-Hes1 (Jensen et al., 2000a), rabbit anti-Ngn3 (Schwitzgebel et al., 2000), guinea pig anti-Insulin (Dako), rabbit anti-Glucagon (Dako), rabbit anti-Somatostatin (Dako), rabbit anti-PP (Dako), rabbit anti-Ghrelin (Kojima et al., 1999), rabbit anti-pHH3 (Cell Signaling Technology), rabbit anti-pan-CK (Santa Cruz), rabbit anti-Amylase (Sigma-Aldrich), rabbit anti-Glut2 (Thorens et al., 1992), mouse anti-ISL1 (Developmental Studies Hybridoma Bank). The slides were washed with PBS the following day and incubated for 2 hr with the following secondary antibodies: biotinylated goat anti-guinea pig IgG; biotinylated goat anti-rabbit IgG, and biotinylated rabbit anti-goat IgG (all from Vector). The slides were then incubated with avidin-biotin complex (ABC) reagent (Vectastain Elite ABC Kit; Vector) for 50 min followed by the addition of diaminobenzidine tetrahydrochloride (DAB) (Dako) as a substrate-chromogen solution. After hematoxylin counterstaining and dehydration, slides were mounted in mounting medium (MGK-S; Matsunami) and pictures were taken using an Axioskop Microscope (Carl Zeiss). Morphometric analyses of pancreas were carried out using the Scion Image analysis program (Scion). The number of islets was calculated, with the definition of an islet as a group of endocrine cells containing at least five visible nuclei. The endocrine cell mass was calculated as the ratio of each hormone-positive cell area to the total area of the pancreas section. An In situ Apoptosis Detection Kit (Takara) was used for TUNEL (terminal deoxynucleotidyl transferase-mediated dUTP nick end labeling) assays, and tissue taken from the involuting mammary gland of a post-lactating female Wistar rat was used as a positive control for apoptosis. Counterstaining of these sections was performed with methyl green. For E15 embryos, in situ hybridization of *Hes1* was carried out using digoxigenin-labeled cRNA probes according to the reported protocol (Tomita et al., 2000).

Analysis of metabolic parameters

Blood glucose values were determined from whole venous blood taken from mouse tails using an automatic glucometer (Glutest Ace, Sanwa Kagaku) or an enzyme colorimetric assay kit (Glucose CII test, Wako). Blood for insulin and amylase was taken by retroorbital bleeds. Plasma insulin levels were measured using an ELISA kit (Morinaga). For glucagon, blood samples were collected into tubes containing EDTA (1 mg/ml blood) and aprotinin (500 KIE/ml blood). For measurements of pancreatic insulin contents, pancreas were quickly dissected, weighed, and frozen in liquid nitrogen. Insulin was extracted by mechanical homogenization in iced acid ethanol. After 24 hr at 4°C, samples were centrifuged, and the supernatant was collected and stored at −20°C. Insulin concentrations were determined by ELISA. Amylase activity was measured according to the Caraway method using a kit (Amylase-Test Wako, Wako). All values are expressed as mean ± standard error.

Supplemental data

Supplemental Data include six figures, Supplemental Results, and Supplemental Experimental Procedures and can be found with this article online at http://www.cellmetabolism.org/cgi/content/full/3/1/59/DC1/.

Acknowledgments

We thank Dr. Douglas A. Melton for providing *Pdx.cre* mice, Dr. Christopher V.E. Wright for anti-Pdx1 Ab, Dr. Michael S. German for anti-Ngn3 Ab, Dr. Bernard Thorens for anti-Glut2 Ab, Dr. Kenji Kangawa for anti-Ghrelin Ab, and Ryoichiro Kageyama for anti-Hes1 Ab. This work was supported by research grants from the Japanese Ministry of Education, Culture, Sports, Science, and Technology and the Japanese Ministry of Health, Labor and Welfare.

Received: August 2, 2005
Revised: October 30, 2005
Accepted: December 16, 2005
Published: January 10, 2006

References

Ahlgren, U., Pfaff, S.L., Jessell, T.M., Edlund, T., and Edlund, H. (1997). Independent requirement for ISL1 in formation of pancreatic mesenchyme and islet cells. Nature *385*, 257–260.

Ahmad, I., Zaqouras, P., and Artavanis-Tsakonas, S. (1995). Involvement of Notch-1 in mammalian retinal neurogenesis: association of Notch-1 activity with both immature and terminally differentiated cells. Mech. Dev. *53*, 73–85.

Apelqvist, A., Li, H., Sommer, L., Beatus, P., Anderson, D.J., Honjo, T., Hrabe de Angelis, M., Lendahl, U., and Edlund, H. (1999). Notch signalling controls pancreatic cell differentiation. Nature *400*, 877–881.

Dominguez-Bendala, J., Klein, D., Ribeiro, M., Ricordi, C., Inverardi, L., Pastori, R., and Edlund, H. (2005). TAT-mediated neurogenin 3 protein transduction stimulates pancreatic endocrine differentiation in vitro. Diabetes *54*, 720–726.

Dor, Y., Brown, J., Martinez, O.I., and Melton, D.A. (2004). Adult pancreatic beta-cells are formed by self-duplication rather than stem-cell differentiation. Nature *429*, 41–46.

Esni, F., Ghosh, B., Biankin, A.V., Lin, J.W., Albert, M.A., Yu, X., MacDonald, R.J., Civin, C.I., Real, F.X., Pack, M.A., et al. (2004). Notch inhibits Ptf1 function and acinar cell differentiation in developing mouse and zebrafish pancreas. Development *131*, 4213–4224.

Gradwohl, G., Dierich, A., LeMeur, M., and Guillemot, F. (2000). Neurogenin3 is required for the development of the four endocrine cell lineages of the pancreas. Proc. Natl. Acad. Sci. USA *97*, 1607–1611.

Gu, G., Dubauskaite, J., and Melton, D.A. (2002). Direct evidence for the pancreatic lineage: NGN3+ cells are islet progenitors and are distinct from duct progenitors. Development *129*, 2447–2457.

Guz, Y., Montminy, M.R., Stein, R., Leonard, J., Gamer, L.W., Wright, C.V.E., and Teitelman, G. (1995). Expression of murine STF-1, a putative insulin gene transcription factor, in β cells of pancreas, duodenal epithelium and pancreatic exocrine and endocrine progenitors during ontogeny. Development *121*, 11–18.

Hald, J., Hjorth, J.P., German, M.S., Madsen, O.D., Serup, P., and Jensen, J. (2003). Activated Notch1 prevents differentiation of pancreatic acinar cells and attenuate endocrine development. Dev. Biol. *260*, 426–437.

Hamada, Y., Kadokawa, Y., Okabe, M., Ikawa, M., Coleman, J.R., and Tsujimoto, Y. (1999). Mutation in ankyrin repeats of the mouse Notch2 gene induces early embryonic lethality. Development *126*, 3415–3424.

Han, H., Tanigaki, K., Yamamoto, N., Kuroda, K., Yoshimoto, M., Nakahata, T., Ikuta, K., and Honjo, T. (2002). Inducible gene knockout of transcription factor recombination signal binding protein-J reveals its essential role in T versus B lineage decision. Int. Immunol. *14*, 637–645.

Heller, R.S., Jenny, M., Collombat, P., Mansouri, A., Tomasetto, C., Madsen, O.D., Mellitzer, G., Gradwohl, G., and Serup, P. (2005). Genetic determinants of pancreatic epsilon-cell development. Dev. Biol. *286*, 217–224.

Hrabé de Angelis, M., McIntyre, J., II, and Gossler, A. (1997). Maintenance of somite borders in mice requires the Delta homologue Dll1. Nature *386*, 717–721.

Ishibashi, M., Ang, S.L., Shiota, K., Nakanishi, S., Kageyama, R., and Guillemot, F. (1995). Targeted disruption of mammalian hairy and Enhancer of split homolog-1 (HES-1) leads to up-regulation of neural helix-loop-helix factors, premature neurogenesis, and severe neural tube defects. Genes Dev. *9*, 3136–3148.

Jensen, J., Pedersen, E.E., Galante, P., Hald, J., Heller, R.S., Ishibashi, M., Kageyama, R., Guillemot, F., Serup, P., and Madsen, O.D. (2000a). Control of endodermal endocrine development by Hes-1. Nat. Genet. *24*, 36–44.

Jensen, J., Heller, R.S., Funder-Nielsen, T., Pedersen, E.E., Lindsell, C., Weinmaster, G., Madsen, O.D., and Serup, P. (2000b). Independent development of pancreatic alpha- and beta-cells from neurogenin3-expressing precursors: a role for the notch pathway in repression of premature differentiation. Diabetes *49*, 163–176.

Kageyama, R., and Ohtsuka, T. (1999). The Notch-Hes pathway in mammalian neural development. Cell Res. *9*, 179–188.

Kato, H., Sakai, T., Tamura, K., Minoguchi, S., Shirayoshi, Y., Hamada, Y., Tsujimoto, Y., and Honjo, T. (1996). Functional conservation of mouse Notch receptor family members. FEBS Lett. *395*, 221–224.

Kojima, M., Hosoda, H., Date, Y., Nakazato, M., Matsuo, H., and Kangawa, K. (1999). Ghrelin is a growth-hormone-releasing acylated peptide from stomach. Nature *402*, 656–660.

Lammert, E., Brown, J., and Melton, D.A. (2000). Notch gene expression during pancreatic organogenesis. Mech. Dev. *94*, 199–203.

Miyamoto, Y., Maitra, A., Ghosh, B., Zechner, U., Argani, P., Iacobuzio-Donahue, C.A., Sriuranpong, V., Iso, T., Meszoely, I.M., Wolfe, M.S., et al. (2003). Notch mediates TGF alpha-induced changes in epithelial differentiation during pancreatic tumorigenesis. Cancer Cell *6*, 565–576.

Murtaugh, L.C., and Melton, D.A. (2003). Genes, signals, and lineages in pancreas development. Annu. Rev. Cell Dev. Biol. *19*, 71–89.

Murtaugh, L.C., Stanger, B.Z., Kwan, K.M., and Melton, D.A. (2003). Notch signaling controls multiple steps of pancreatic differentiation. Proc. Natl. Acad. Sci. USA *100*, 14920–14925.

Oka, C., Nakano, T., Wakeham, A., de la Pompa, J.L., Mori, C., Sakai, T., Okazaki, S., Kawaichi, M., Shiota, K., Mak, T.W., and Honjo, T. (1995). Disruption of the mouse RBP-J kappa gene results in early embryonic death. Development *121*, 3291–3301.

Pang, K., Mukonoweshuro, C., and Wong, G.G. (1994). Beta cells arise from glucose transporter type 2 (Glut2)-expressing epithelial cells of the developing rat pancreas. Proc. Natl. Acad. Sci. USA *91*, 9559–9563.

Pictet, R., and Rutter, W.J. (1972). Development of the embryonic endocrine pancreas. In Handbook of Physiology, Section 7, D.F. Steiner and N. Frenkel, eds. (Baltimore, MD: Williams and Williams), pp. 25–66.

Pui, J.C., Allman, D., Xu, L., DeRocco, S., Karnell, F.G., Bakkour, S., Lee, J.Y., Kadesch, T., Hardy, R.R., Aster, J.C., and Pear, W.S. (1999). Notch1 expression in early lymphopoiesis influences B versus T lineage determination. Immunity *11*, 299–308.

Schwitzgebel, V.M., Scheel, D.W., Conners, J.R., Kalamaras, J., Lee, J.E., Anderson, D.J., Sussel, L., Johnson, J.D., and German, M.S. (2000). Expression of neurogenin3 reveals an islet cell precursor population in the pancreas. Development *127*, 3533–3542.

Swiatek, P.J., Lindsell, C.E., del Amo, F.F., Weinmaster, G., and Gridley, T. (1994). Notch1 is essential for postimplantation development in mice. Genes Dev. *15*, 707–719.

Thorens, B., Wu, Y.J., Leahy, J.L., and Weir, G.C. (1992). The loss of GLUT2 expression by glucose-unresponsive cells of db/db mice is reversible and is induced by the diabetic environment. J. Clin. Invest. *90*, 77–85.

Tomita, K., Moriyoshi, K., Nakanishi, S., Guillemot, F., and Kageyama, R. (2000). Mammalian achaete-scute and atonal homologs regulate neuronal versus glial fate determination in the central nervous system. EMBO J. *19*, 5460–5472.

Wilson, A., MacDonald, H.R., and Radtke, F. (2001). Notch 1-deficient common lymphoid precursors adopt a B cell fate in the thymus. J. Exp. Med. *194*, 1003–1012.

Xue, Y., Gao, X., Lindsell, C.E., Norton, C.R., Chang, B., Hicks, C., Gendron-Maguire, M., Rand, B., Weinmaster, G., and Gridley, T. (1999). Embryonic lethality and vascular defects in mice lacking the Notch ligand Jagged1. Hum. Mol. Genet. *8*, 723–730.

Diabetologia
DOI 10.1007/s00125-006-0193-8

ARTICLE

T. Tomita · H. Masuzaki · H. Iwakura · J. Fujikura · M. Noguchi · T. Tanaka · K. Ebihara · J. Kawamura · I. Komoto · Y. Kawaguchi · K. Fujimoto · R. Doi · Y. Shimada · K. Hosoda · M. Imamura · K. Nakao

Expression of the gene for a membrane-bound fatty acid receptor in the pancreas and islet cell tumours in humans: evidence for GPR40 expression in pancreatic beta cells and implications for insulin secretion

Received: 3 August 2005 / Accepted: 23 December 2005

Abstract *Aims/hypothesis* G protein-coupled receptor 40 (GPR40) is abundantly expressed in pancreatic beta cells in rodents, where it facilitates glucose-induced insulin secretion in response to mid- to long-chain fatty acids in vitro. However, *GPR40* gene expression in humans has not been fully investigated, and little is known about the physiological and pathophysiological roles of GPR40 in humans. The aim of this study, therefore, was to examine GPR40 expression and its clinical implications in humans. *Methods: GPR40* mRNA expression in the human pancreas, pancreatic islets and islet cell tumours was analysed using TaqMan PCR. *Results: GPR40* mRNA was detected in all human pancreases collected intraoperatively. It was enriched approximately 20-fold in isolated islets freshly prepared from the pancreases of the same individuals. The estimated mRNA copy number for the *GPR40* gene in pancreatic islets was comparable to those for genes encoding sulfonylurea receptor 1, glucagon-like peptide 1 receptor and somatostatin receptors, all of which are known to be expressed abundantly in the human pancreatic islet. A large amount of *GPR40* mRNA was detected in insulinoma tissues, whereas mRNA expression was undetectable in glucagonoma or gastrinoma. The *GPR40* mRNA level in the pancreas correlated with the insulinogenic index, which reflects beta cell function (r=0.82, p=0.044), but not with glucose levels during the OGTT, the insulin area under the OGTT curve or the index for the homeostasis model assessment of insulin resistance (HOMA-IR). *Conclusions/interpretation* The present study provides evidence for *GPR40* gene expression in pancreatic beta cells and implicates GPR40 in insulin secretion in humans.

Keywords Human · GPR40 · Pancreas · Pancreatic islets · Insulinoma · Insulin secretion

Abbreviations GLP1R: glucagon-like peptide 1 receptor · GPR40: G protein-coupled receptor 40 · GSIS: glucose-stimulated insulin secretion · HOMA-IR: homeostasis model assessment of insulin resistance · SSTR: somatostatin receptor · SUR1: sulfonylurea receptor 1

T. Tomita · H. Masuzaki (✉) · H. Iwakura · J. Fujikura · M. Noguchi · T. Tanaka · K. Ebihara · K. Hosoda · K. Nakao
Department of Medicine and Clinical Science,
Kyoto University Graduate School of Medicine,
54 Shogoin Kawahara-cho, Sakyo-ku,
Kyoto 606-8507, Japan
e-mail: hiroaki@kuhp.kyoto-u.ac.jp
Tel.: +81-75-751-3172
Fax: +81-75-771-9452

J. Kawamura · I. Komoto · Y. Kawaguchi · K. Fujimoto · R. Doi · Y. Shimada · M. Imamura
Department of Surgery and Surgical Basic Science,
Kyoto University Graduate School of Medicine,
Kyoto, Japan

Introduction

Fatty acids play a pivotal role in a variety of metabolic controls and cell signalling processes in various tissues [1]. In particular, short-term exposure of fatty acids to pancreatic beta cells augments glucose-stimulated insulin secretion (GSIS), a process in which fatty acid-derived metabolites such as long-chain fatty acyl-CoAs act as crucial effectors [2]. However, the entire mechanism whereby fatty acids acutely induce GSIS augmentation has not been fully elucidated [3]. In contrast, chronic fatty acid exposure causes marked deterioration of beta cell function, which is referred to as lipotoxicity [4, 5].

Several investigators have recently demonstrated that fatty acids act as ligands for membrane-bound G-protein-coupled receptors such as GPR40 [3, 6, 7], GPR41, GPR43 [8, 9] and GPR120 [10]. GPR40 is preferentially expressed in pancreatic beta cells in rodents and augments GSIS after acute exposure to mid- and long-chain fatty acids [6]. Silencing GPR40 with the small interfering RNA (siRNA) system suppresses long-chain fatty acid-induced GSIS augmentation in pancreatic beta cells [6]. A recent study of

GPR40 knockout mice and beta-cell-specific GPR40 transgenic mice suggested a physiological and pathophysiological role for GPR40 in insulin secretion and diabetes mellitus [11]. Although these findings implicate GPR40 in insulin secretion and glucose metabolism in rodents, little is known about the physiological significance of GPR40 in humans.

In this context, we investigated *GPR40* gene expression in the pancreas and in islet cell tumours collected during surgery. We also explored the potential role of GPR40 in beta cell function in humans.

Subjects and methods

Participants, tissue sampling and pancreatic islet preparation

Seventeen patients with pancreatic tumours provided written informed consent to participation in the present study, which was approved by the Ethical Committee on Human Research of Kyoto University Graduate School of Medicine (No. 508, 2003), and conducted according to the principles of the Declaration of Helsinki. Table 1 summarises the patient profiles. Patients who underwent pancreatectomy (patients 1–12) were numbered according to the *GPR40* mRNA level in the pancreas. None of the 12 patients were treated with oral glucose-lowering agents or insulin. Pancreatic, intestinal and hepatic tissues free of tumour invasion as well as islet cell tumour tissues were obtained at the time of surgery (Table 1). Islet tissues from three patients (patients 9–11) were promptly isolated from the pancreas through the mince method [12]. Briefly, the pancreas was finely minced by hand for 15–30 min on ice and digested at 37°C with 600 IU/ml of type V collagenase (Sigma, St Louis, MO, USA) in Hanks' Balanced Salt Solution (HBSS) containing 1% bovine serum albumin (Fraction V, Sigma) for 20 min. The digested tissue was washed three times in cold HBSS. After dithizone staining, pancreatic islets were manually collected using a stereo microscope (SZ-STB1; Olympus, Tokyo, Japan).

Quantification of mRNA expression of *GPR40* and other receptor genes

We measured mRNA expression of the *GPR40* gene as well as genes encoding sulfonylurea receptor 1 (*ABCC8*, previously known as *SUR1*) [13], glucagon-like peptide 1 receptor (*GLP1R*) [14, 15] and somatostatin receptor (*SSTR*) 3 and 5 [16] using the following method. Total RNA was extracted using the Qiagen RNeasy Mini Kit (Qiagen, Hilden, Germany) [17]. First-strand cDNA was synthesised by random hexamer-primed reverse transcription using SuperScript II reverse transcriptase (Invitrogen, Carlsbad, CA, USA) [18]. The mRNA level was quantified by the TaqMan PCR method using an ABI Prism 7700 Sequence Detector (Applied Biosystems, Foster City, CA, USA) as described [19]. To calculate the copy number of each mRNA, standard curves were generated using synthesised oligo DNA fragments (Proligo Japan, Kyoto, Japan) containing the PCR amplicon region. The mRNA expression in each gene was normalised to that of *GAPDH* (i.e. the mRNA level for each gene was expressed as

Table 1 Clinical profiles of patients and tissues

Patient number	Age (years)	Sex (M/F)	Disease	Tissue analysed
1	53	F	Pancreatic cancer	Pancreas (head)/duodenum
2	47	F	Pancreatic cancer	Pancreas (head)/jejunum
3	71	F	Pancreatic cancer	Pancreas (body)
4	59	F	Insulinoma	Pancreas (head)/insulinoma
5	72	F	Pancreatic cancer	Pancreas (head)/jejunum
6	75	M	Pancreatic cancer	Pancreas (head)/duodenum/jejunum
7	45	M	Gastrinoma	Pancreas (body)
8	63	F	Islet cell tumour (non-functional)	Pancreas (body)
9	60	M	Pancreatic cancer	Pancreas (body)
10	63	M	Pancreatic cancer	Pancreas (head)
11	54	M	Pancreatic cancer	Pancreas (head)
12	55	F	Pancreatic cancer	Pancreas (body)
13	64	F	Liver metastasis (glucagonoma)	Liver
14	54	F	Insulinoma	Insulinoma
15	30	M	Insulinoma	Insulinoma
16	23	F	Glucagonoma	Glucagonoma
17	56	M	Gastrinoma	Gastrinoma

Patients were premedicated with 0.01 mg/kg atropine sulphate i.m. and 0.2 mg/kg diazepam orally before surgery
Tissues were sampled under general anaesthesia with 35% O_2, 65% N_2O and 0.5–1.5% sevoflurane. Neuromuscular blockade was provided with vecuronium bromide; initial dose 0.1 mg/kg, supplemented as required

receptor/*GAPDH* [copy/copy]). Table 2 summarises the sequences of primers and probes used in the present study. The primers or probes were designed not to cover any reported single-nucleotide polymorphisms [20–23].

Data analysis on glucose homeostasis

The insulin AUC was calculated using the trapezoidal rule from OGTT data. We evaluated beta cell function and systemic insulin resistance using the insulinogenic index (n=7) and the homeostasis model assessment of insulin resistance (HOMA-IR) (n=10), respectively. The insulinogenic index was calculated as the ratio of the insulin concentration (pmol/l) increment to the glucose concentration (mmol/l) increment at 30 min into the OGTT (Δ30insulin/Δ30glucose) [24]. HOMA-IR was calculated in fasting conditions as plasma insulin (pmol/l)×blood glucose (mmol/l)/22.5 [25, 26]. The difference in the patient numbers for the two indices is based on the difference in data availability, such as blood glucose and insulin levels at 30 min during the OGTT.

Statistical analysis

The relationship between the *GPR40* mRNA level in the pancreas and clinical or metabolic profiles was tested using Spearman's rank correlation and a p value of less than 0.05 was considered significant. The statistical significance of differences in two groups was assessed using unpaired two-tailed t-test and a p value of less than 0.05 was considered significant (Statcel, Social Research Information, Tokyo, Japan).

Results

Expression of *GPR40* mRNA in human pancreas and isolated islets

The expression of *GPR40* mRNA in human tissues was assessed by TaqMan PCR using total RNA samples from patients who underwent pancreatectomy and/or other pertinent surgeries. *GPR40* mRNA was detected in all human pancreases examined (n=12), and at higher levels than those in the duodenum, jejunum or liver (Fig. 1a). The inter-individual variability in the *GPR40* mRNA levels was considerable in the human pancreas. The *GPR40* mRNA level in the pancreas was not significantly different between sites (head vs body) of the pancreas or between men and women. The *GPR40* mRNA level in the pancreas did not correlate significantly with age. The *GPR40* mRNA level in fresh islets that were isolated from pancreatic tissues (n=3) was approximately 20-fold higher than that in the pancreas from the same patients (Fig. 1b).

To gain further insight into the expression of the *GPR40* gene in pancreatic islets, we analysed the expression of genes known to be expressed abundantly in the pancreatic islets. The estimated mRNA copy number of the *GPR40* gene in isolated islets was comparable to or higher than those of genes encoding receptors for sulfonylurea, glucagon-like peptide 1 and somatostatin (Fig. 1c), suggesting that high levels of the *GPR40* gene are expressed in pancreatic islets.

Expression of *GPR40* mRNA in insulinoma tissues

We analysed the expression of *GPR40* mRNA in islet cell tumours, including insulinoma (n=3), glucagonoma (n=1)

Table 2 Sequences of TaqMan primers and probes

Gene	Forward primer (5′→3′)	Probe (FAM-5′→3′-TAMRA)	Reverse Primer (5′→3′)	Accession number
GPR40	GCCCGCTTCAGCC TCTCT	TCTGCCCTTGGCCATCA CAGCCT	GAGGCAGCCCAC GTAGCA	NM_005303
GLP1R	GCAGCCCTGAAGTGG ATGTATAG	ACAGCCGCCCAGCAGCA CCAGT	CTCAGAGAGTCCT GGTAGGAGAG	NM_002062
ABCC8	GCTGCCCATCGTTATG AGGG	CCTCACCAACTACCAACG GCTCTGCG	GAATGTCCTTCCG CACCTGG	NM_000352
SSTR3	CCGTCAGTGGCGTTCT GATCC	CCACCACGCACACCACC AGGTAGACC	ATAGATGACCAGC GAGTTACCCAG	NM_001051
SSTR5	CTCGGAGCGGAAGGT GACG	AACACCAGCACCACCACCAA CACCAT	GTGAAGAAGGGCA GCCAACATC	NM_001053
GAPDH	TGAAGCAGGCGTCGG AGG	CCTCAAGGGCATCCTGGGCTA CACTG	GCTGTTGAAGTCAG AGGAGACC	NM_002046

The *ABCC8* gene is also known as *SUR1* and encodes sulfonylurea receptor 1
FAM 6-carboxyfluorescein, *TAMRA* 6-carboxytetramethylrhodamine

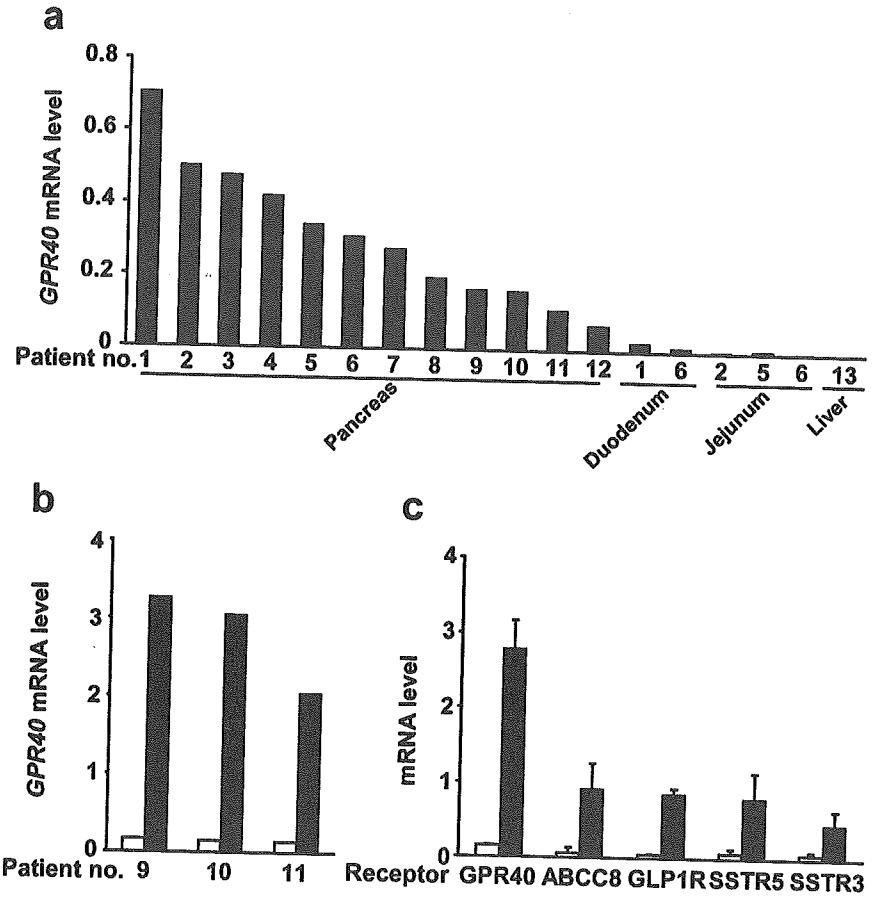

Fig. 1 TaqMan quantitative analyses of *GPR40* mRNA expression in human pancreatic tissues. Total RNA extracted from various tissues was analysed. **a** *GPR40* mRNA was detected in all human pancreas specimens examined, at higher abundance than in the duodenum, jejunum or liver. Patients 1–12 were numbered according to their relative level of expression of *GPR40* mRNA. **b** *GPR40* mRNA level in isolated islets was ~20-fold higher than in pancreatic tissues from the same patients. The numbers in **a** and **b** correspond to those in Table 1. **c** Estimated mRNA copy number of the *GPR40* gene was similar to or higher than those for genes encoding sulfonylurea receptor 1 (*ABCC8*), glucagon-like peptide 1 receptor (*GLP1R*) and somatostatin receptors 3 (*SSTR3*) and 5 (*SSTR5*) (n=3). Data are means±SEM. *Open bars* pancreas; *closed bars* isolated islets

and gastrinoma (n=1). *GPR40* mRNA was detected in tissue extracts from three cases of insulinoma (Fig. 2), which was comparable to that in pancreatic islets (Fig. 2). *GPR40* mRNA was below detectable levels in tissue extracts from glucagonoma or gastrinoma (Fig. 2).

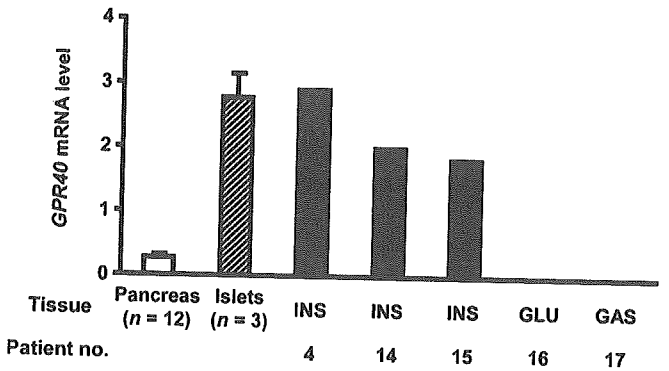

Fig. 2 TaqMan quantitative analyses of *GPR40* mRNA expression in human islet cell tumours. Total RNA extracted from pancreases (n=12), pancreatic islets (n=3) and islet cell tumours (patients 4, 14, 15, 16, 17) was analysed. *GPR40* mRNA was abundantly expressed in three cases of insulinoma among islet cell tumours. *Open bar*, pancreas; *hatched bar*, pancreatic islets; *closed bars*, islet cell tumours. The patient numbers in the figure correspond to those in Table 1. The *GPR40* mRNA level in the pancreas and pancreatic islets is expressed as mean±SEM. *INS* insulinoma, *GLU* glucagonoma, *GAS* gastrinoma

The correlation between the *GPR40* mRNA level in the pancreas and insulinogenic index is positive

To understand the physiological role of GPR40 in humans, we examined the relationship between the *GPR40* mRNA level in the pancreas and various metabolic parameters. Table 3 summarises the metabolic profiles of patients who underwent pancreatectomy. The *GPR40* mRNA level in the pancreas did not correlate significantly with BMI, fasting plasma glucose, plasma glucose at 2 h under the OGTT (2h-PG) or insulin AUC. Furthermore, the *GPR40* mRNA level in the pancreas did not correlate significantly with the HOMA-IR (n=10) (Fig. 3a). The significant positive correlation between the *GPR40* mRNA level in the pancreas and the insulinogenic index was notable (n=7) (p=0.044, r=0.82) (Fig. 3b). To verify the significant association, correlation was tested between the *GPR40* mRNA level in the pancreas and the HOMA-IR, using data from the same patients from whom data on the insulinogenic index were available (n=7), and we confirmed that there was no significant correlation between the *GPR40* mRNA level and the HOMA-IR (p=0.86, r=0.07). The *GPR40* mRNA level in the pancreas was not significantly associated with HbA_{1c} or fasting triglyceride.